Journal of Biological Research

Bollettino della Società Italiana di Biologia Sperimentale

eISSN 2284-0230 - pISSN 1826-883

https://www.pagepressjournals.org/index.php/jbr/index

J Biol Res 2026 [Online ahead of print]

To cite this Article:

Basset CA, Dosh L, Hussein IH, et al. **The role of heat shock protein chaperones in human and murine salivary gland ontogenesis.** *J Biol Res* doi: 10.4081/jbr.2026.14820

Submitted: 5 January 2026

Accepted: 25 April 2026

Early access: 10 July 2026

The role of heat shock protein chaperones in human and murine salivary gland ontogenesis

Charbel A. Basset,[1] Laura Dosh,[2] Inaya Hajj Hussein,[3] Rosalyn Jurjus,[2] Francesca Rappa,[1,4] Lavinia Giovanna Leone,[5] Maria Laura Uzzo,[1] Giovanni Francesco Spatola,[1] Giuseppe Vergilio,[1,6] Abdo Jurjus,[2] Angelo Leone[1]

[1]Department of Biomedicine, Neuroscience and Advanced Diagnostics, Institute of Human Anatomy and Histology, University of Palermo, Italy; [2]Department of Anatomy, Cell Biology and Physiology, Faculty of Medicine, American University of Beirut, Lebanon; [3]Department of Foundational Medical Studies, OUWB School of Medicine, Michigan, USA; [4]Institute of Translational Pharmacology, National Research Council of Italy (CNR), Palermo, Italy; [5]School of Medicine, University of Palermo, Palermo, Italy; [6]Department of Neurosurgery, National Relevance and Specialization Hospital Trust ARNAS Civico, Palermo, Italy

Correspondence: Angelo Leone, Department of Biomedicine, Neuroscience and Advanced Diagnostics, Institute of Human Anatomy and Histology, University of Palermo, Italy. E-mail: angelo.leone@unipa.it

Giuseppe Vergilio, Department of Biomedicine, Neuroscience and Advanced Diagnostics, Institute of Human Anatomy and Histology, University of Palermo, Italy. E-mail: giuseppe.vergilio@unipa.it

Key words: chaperone system; salivary glands; ontogenesis; Heat Shock Proteins (Hsps) mapping.

Abstract

The chaperone system plays essential roles in health and disease and is likely critical during embryogenesis. Previous studies have focused on early stages, from the one-cell stage to the

blastocyst, with no information available on the topographic distribution or quantitative expression of chaperone system components, such as molecular chaperones, after the blastocyst stage in salivary glands. This study aims to map the distribution and expression levels of key molecular chaperones, including Heat Shock Proteins (Hsps), in embryonic salivary glands of mice and humans. Tissue levels of Hsp10, Hsp60, and Hsp90 in humans and mice, Hsp27 in humans, and Hsp25 in mice were assessed by immunohistochemistry in adult and embryonic paraffin-embedded salivary gland tissues. Protein and gene expression of Hsps were further analyzed in adult mouse submandibular glands. All studied Hsps were present at substantial levels in embryonic salivary gland tissues of both species. Immunohistochemical analysis revealed a developmental shift in Hsp distribution: with development, Hsps were predominantly confined to the ducts. In conclusion, this study provides a first descriptive and quantitative map of chaperone system components in human salivary gland development. The stage-dependent differences observed between embryonic and adult tissues offer a reference framework that may inform future functional investigations into salivary gland morphogenesis and related pathological conditions.

Introduction

Salivary gland development occurs through branching morphogenesis, a multistep process involving epithelial–mesenchymal interactions, epithelial arborization, and repeated cycles of rearrangement and reorganization of newly formed end buds that ultimately give rise to ductal and acinar structures. In humans, this process begins between the 4th and 6th week of gestation and is completed by the 6th month.[1-3] In mouse salivary glands, the initial bud stage occurs between embryonic days E1.5 and E12, and by E17 the fully lumenized acini are connected to the oral cavity through a mature ductal network.[4] Despite species-specific differences in timing, the conserved morphological sequence of salivary gland morphogenesis makes the human–mouse comparison particularly informative for identifying shared developmental principles.

Recent evidence indicates the involvement of the Chaperone System (CS) in tissue branching morphogenesis, particularly in neurodevelopment and epidermal development and differentiation.[5-7] The CS comprises molecular chaperones, chaperone co-factors, co-chaperones, and chaperone interactors and receptors within an organism.[8] Owing to its fundamental role in maintaining protein homeostasis and buffering the deleterious effects of stressors at the molecular, cellular, and tissue levels, the CS is thought to have emerged early in evolution. CS components are ubiquitously expressed but show marked tissue- and stage-specific differences in composition and abundance.

Our laboratories have previously investigated the CS in salivary glands, a tissue for which information remains limited despite its relevance in health and disease.[9-13] Early studies described the expression patterns of Hsp70/DnaK, Hsp60/DnaJ, and CCT chaperone families in several human tissues, including salivary glands.[14,15] Subsequent work extended these observations to Hsp90 and the small heat shock protein Hsp27, primarily focusing on adult human salivary glands.[9-12] Here, we build upon this body of work by extending the analysis to embryonic stages in both humans and mice.

During ontogenesis, cell proliferation reaches its peak, leading to a marked increase in nascent polypeptides that require efficient folding and quality control to support tissue growth and morphogenesis. In this context, molecular chaperones are expected to play a critical role in sustaining epithelial expansion, lumen formation, and the progressive differentiation of ductal and acinar compartments. A substantial body of evidence supports the requirement of Heat Shock Proteins (Hsps) during mammalian embryonic development.[16]

Constitutive members of the Hsp70 family, such as Heat Shock Cognate 70 (Hsc70), together with inducible Hsp70 and the co-chaperone Hsp40, have been detected in soluble and insoluble fractions of embryonic chicken lens, cornea, and ciliary body as early as E12.[17] Constitutive Hsc70 and Hsp90β, as well as the small heat shock protein Hsp27 and T-complex protein 1 subunit alpha (TCP-1α), are present in the developing mouse brain at early ontogenetic stages (E9.5 and E12.5) (18). Inducible Hsp70 and Hsp90α appear later (E15.5), albeit at lower levels than their constitutive counterparts.[18] Although tissue levels of constitutive and inducible Hsps vary, they display distinct spatial distribution patterns, with the notable exception of Hsp90β, which shows near-ubiquitous expression.[18] Hsp70 expression increases progressively from E12.5 to late gestational stages (E17) in the mouse embryo.[19]

Endoplasmic Reticulum (ER)-resident chaperones also play a pivotal role during development. Glucose-Regulated Protein 78 (GRP78) is highly expressed at early stages of embryogenesis and subsequently declines during later stages of heart development,[20,21] while GRP94 exhibits similarly elevated expression in embryonic heart, neuroepithelium, and surface ectoderm tissues.[22] Knockout of either ER chaperone leads to severe morphological abnormalities and embryonic lethality.[23] These findings highlight the importance of ER proteostasis during periods of intense secretory and structural remodeling, such as those characterizing ductal and acinar differentiation.

Most available studies have focused on pre-implantation stages, particularly from the two-cell stage to blastocyst formation.[24,25] Consequently, the roles of Hsps during mid- to late-stage embryonic development remain poorly understood, and data on salivary gland development are entirely lacking. Given the secretory nature of salivary glands and the progressive establishment of polarized epithelial structures, the targeted analysis of selected Hsps involved in cytosolic folding, cytoskeletal organization, and ER homeostasis is biologically justified.

The aim of this study is therefore to descriptively assess and map the distribution of key CS components in human and murine salivary glands during ontogenesis. The parallel analysis of the two species provides a conceptual and comparative framework that supports the use of a schematic summary to highlight conserved and divergent patterns across developmental stages.

Materials and Methods

Human embryo specimen

Human 13-week gestation (13w) head sections were obtained from the archives of the Department of Anatomy and Histology, University of Palermo, Palermo.

Mouse specimens

All animal work was conducted according to institutional guidelines and approved by the American University of Beirut (AUB) Institutional Animal Care and Use Committee (IACUC), Lebanon (IACUC#19-10-555). Eight-month-old male FVB/NJ mice and C57BL/6 mouse embryos were used to investigate the expression and localization patterns of molecular chaperones in salivary glands at embryonic and adult stages.

Submandibular Salivary Gland (SMG) surgical excision

FVB/NJ mice (n=6) were euthanized by isoflurane-induced anesthesia followed by cervical dislocation. The mice were fixed on the operating board in the dorsal position with the tail toward the investigator. Before incision, 70% ethanol was applied to the neck and chest to reduce contamination. A midline skin incision was made from above the suprasternal notch to the lower jaw. This incision was extended laterally from the suprasternal notch to both shoulders, followed by blunt dissection to detach the skin from the underlying glands, fat, and muscles. The skin was then retracted with forceps and secured with hypodermic needles to expose the neck region. The superficial cervical lymph nodes with attached connective tissue were removed. Fat and connective tissue surrounding each salivary gland were dissected away. The submandibular glands were separated from underlying tissue, lifted with iris forceps, and cut from the base using iris scissors. Each gland was placed in cold phosphate-buffered saline (PBS, Corning, Manassas, VA, USA) on a pre-chilled tissue culture plate. One gland was fresh-frozen in liquid nitrogen and stored at –80°C for molecular analyses, while the other was fixed in 10% paraformaldehyde for 48 hours and embedded in paraffin for morphological studies.

Mouse embryo harvest

Six C57BL pregnant mice at 16 days of gestation (E16) were euthanized by isoflurane anesthesia followed by cervical dislocation. The midsection skin was lifted with forceps and incised along the ventral midline. The skin was separated from the abdominal and thoracic walls, and another incision opened the abdominal cavity. Uterine sacs containing strings of embryos were removed, and embryos were released by cutting through the outer membrane.

Embryos were placed in cold PBS on a tissue culture plate under an SMZ stereomicroscope (Nikon Corporation. Tokyo, Japan). Embryo heads were harvested with iris scissors and fixed in 10% paraformaldehyde for 48 hours before paraffin embedding. Embryos were collected at embryonic day 16 (E16) (equivalent to 13 weeks of human gestation), a stage at which salivary glands are already formed.

Histopathology

Embryo heads and Adult Mouse (AM) salivary gland sections (5 µm) were obtained from paraffin blocks and stained with hematoxylin–eosin (H&E) for histological examination. Sections were de-waxed in xylene for 10 minutes, rehydrated in decreasing ethanol concentrations, stained with H&E,[26] and analyzed using a Leica DM5000 upright microscope (Leica Microsystems, Heidelberg, Germany). Sections were examined by two independent observers (A.L. and A.J.) blinded to sample identity.

Immunohistochemistry

Immunohistochemistry (IHC) for Hsp10, Hsp27, Hsp60, and Hsp90 was performed on 5-7 µm paraffin-embedded sections of AM salivary gland and mouse embryo heads using the automated IntelliPath Flx IHC system (Biocare Medical Pacheco, CA, USA). Nuclear counterstaining was done with hematoxylin (DAKO, Cat. S2020, Glostrup, Denmark). Slides were re-dehydrated in ascending alcohol concentrations and cleared in xylene. Coverslips were mounted with aqueous mounting medium. Tissue sections were examined using a DM5000 B microscope with a DC 300 F camera (Leica, Wetzlar, Germany). Each section was evaluated twice by two independent observers (A.L. and A.J.). The percentage of Hsp-positive cells was assessed in high-power fields (HPFs, 400×), repeated for 10 HPFs, and averaged for statistical analyses. Primary antibodies used included anti-Hsp10 (mouse monoclonal antibody D-8, sc-376313, 1:100), anti-Hsp27 (mouse monoclonal antibody, F-4, sc-13132, 1:200), anti-Hsp60 (rabbit polyclonal antibody H-300, sc-13966, 1:200), and anti-Hsp90 (mouse monoclonal antibody, sc-13119, 1:200) all from Santa Cruz Biotechnology (Dallas, USA). Manual quantification was used instead of ImageJ because software cannot

reliably distinguish true immunopositivity from background or differentiate salivary gland cells from stromal cells. Quantification was performed by two pathologists experienced in chaperonopathies, following established methods.[27-30]

Positive standards

Positivity for each chaperone was assessed based on: i) percentage of positive cells (<5% = negative); ii) staining intensity, rated + (weak) to +++ (strong), following established criteria.[30]

Western blot

AM SMG tissue was lysed in Radio Immuno-Precipitation Assay (RIPA) buffer containing 0.1% SDS (Merck/Sigma-Aldrich, St. Louis, MO, USA), 0.5% sodium deoxycholate (Merck/Sigma-Aldrich, St. Louis, MO, USA), 150 mM NaCl (Merck/Sigma-Aldrich, St. Louis, MO, USA), 100 mM Ethylenediaminetetraacetic acid (EDTA) (Thermo Fisher Scientific, Waltham, MA, USA), 50 mM Tris-HCl, 1% NP-40 (Thermo Fisher Scientific, 168 Third Avenue, Waltham, MA 02451, USA), protease inhibitors (MilliporeSigma, Darmstadt, Germany), and 1 mM Phenylmethylsulfonyl Fluoride (PMSF) (Thermo Fisher Scientific, 168 Third Avenue, Waltham, MA 02451, USA). Lysates were centrifuged at 13,600 rpm for 30 minutes at 4°C.[31] For immunoblotting, 40 µg protein was separated on 10–15% polyacrylamide gels (Bio-Rad Laboratories, Inc., Hercules, CA 94547, USA.) and transferred to nitrocellulose membranes. Blots were blocked with 5% Bovine Serum Albumin (BSA) Sigma-Aldrich St. Louis USA or 5% milk in Tris-Buffered Saline (TBS) Sigma-Aldrich St. Louis USA and incubated overnight with rabbit polyclonal anti-Hsp10 (sc-20958, FL-102, 1:1000) or anti-Hsp60 (sc-13966, H-300, 1:2000). Horseradish Peroxidase (HRP)-conjugated Sigma-Aldrich St. Louis USA) secondary antibodies (Bio-Rad Laboratories, Inc., Hercules, CA 94547, USA, 1:1000) were used for detection by enhanced chemiluminescence. Densitometry was performed using ImageJ.[32]

RNA Preparation and Quantitative Real-Time PCR (RT-PCR)

mRNA expression in AM SMG was analyzed using SYBR Green real-time Polymerase Chain Reaction and ΔΔCt method.[33] Total RNA was isolated using TRIzol (Sigma Aldrich, Saint Louis, USA) and reverse-transcribed using the QuantiTect Reverse Transcription Kit (Qiagen, Hilden, Germany). cDNA was amplified on a CFX384 system (Bio-Rad Laboratories, Inc. Hercules, USA) using SYBR Green. Primers for Hsp10, Hsp27, and Hsp60 were used, with 26S rRNA as the reference gene (Table 1). All samples were run in duplicate using 2 µl of cDNA per reaction.

Statistical evaluation

All experiments were repeated at least in triplicate, and all data are presented as mean ± Standard Deviation (SD). One-way Analysis of Variance (ANOVA) was used for statistical analysis (GraphPad Prism, GraphPad Software, San Diego, CA, USA); p values ≤ 0.05 were considered statistically significant.

Results

We assessed the expression of Hsp10, Hsp27, Hsp60, and Hsp90 at mid-stage salivary gland development in humans and mice, and subsequently compared these findings with expression patterns in adult glands. The levels of immunohistochemical positivity (percentage of positive cells and reaction intensity) for each chaperone in adult and embryonic human and mouse SMG are summarized in Table 2. Chaperone expression in adult human SMG has been previously described.[9-12]

Illustrative images of the immunohistochemical mapping of the four chaperones are shown in Figure 1**.** The main observations are as follows:
Hsp10 demonstrated granular and diffuse cytoplasmic positivity across all specimens. In AM SMG, ductal cells exhibited low to high reaction intensity, whereas acinar cells showed markedly lower positivity, ranging from negative to moderate (Figure 1e). In the 16-day mouse embryo (E16), a moderate to high epithelial intensity was observed (Figure 1f). In

contrast, the human 13-week embryo (13w) exhibited comparatively weaker Hsp10 positivity (Figure 1h).

Microscopic evaluation of Hsp27 demonstrated diffuse cytoplasmic positivity in all samples. In AM SMG, ducts and myoepithelial cells showed low to intense cytoplasmic staining, whereas acini were negative (Figure 1i). In E16 glands, staining intensity ranged from weak to strong (Figure 1j), whereas 13w glands showed mild to moderate positivity (Figure 1l).

Hsp60 immunostaining displayed granular and diffuse cytoplasmic positivity across specimens. In AM SMG, ductal cells showed weak to moderate intensity, while acinar cells were negative (Figure 1m). E16 epithelium exhibited predominantly granular cytoplasmic staining with moderate to high intensity (Figure 1n). In 13w tissue, immunopositivity was consistently strong (Figure 1p).
Hsp90 demonstrated diffuse cytoplasmic positivity in all specimens. AM SMG ducts and serous acini showed the strongest intensity of all chaperones examined (Figure 1q). E16 glands exhibited variable staining ranging from weak to strong (Figure 1r), while 13w samples showed uniformly high positivity (Figure 1t).

To complement the immunomorphological findings, we quantified protein levels of Hsp10 and Hsp60 and examined gene transcription levels of *HSP10*, *HSP25* (the murine ortholog of Hsp27), and Hsp60 in AM SMG. Hsp10 protein and gene expression were significantly higher than those of Hsp60 ($p = 0.0020$) (Figure 2a, b), consistent with the immunohistochemical patterns. Among the three chaperones, Hsp25 mRNA expression was lowest, significantly lower than both Hsp10 ($p < 0.0001$) and Hsp60 ($p = 0.0062$) (Figure 2b).

Discussion

The Chaperone System (CS) is a primary homeostatic mechanism in ontogenesis; the early, regulated expression of Hsps from gametogenesis through embryogenesis underscores their essential role in maintaining cellular viability during rapid developmental transitions.[24] While Hsp expression is well-characterized during pre-implantation, its spatio-quantitative distribution during post-implantation and organogenesis remains under-investigated. Initial murine development is under maternal control, with Hsp gene expression being undetectable

at the transcriptionally silent one-cell stage and initiating constitutively only upon zygotic genome activation at the early two-cell stage.[24,25] Inducible Hsp70 appears at the early blastocyst stage and has been implicated both in the initiation of embryonic genome expression[24,25] and in functional blastocyst formation.[23,24] In parallel, Hsp90β has been shown to be indispensable for placental development in mice, further supporting a key role for molecular chaperones in early embryonic organization.[35]

Only a limited subset of molecular chaperones, are component of the CS, has been investigated in the context of murine organogenesis, and comparable data for salivary glands have been largely absent. Within this framework, our study provides a direct comparative analysis of human and murine salivary gland development, allowing shared and species-specific patterns of CS expression to be identified. Our findings indicate that Hsp10, Hsp27, Hsp60, and Hsp90 are all expressed during murine salivary gland morphogenesis at E16. The concurrent presence of these chaperones at a stage characterized by active branching morphogenesis and ductal–acinar differentiation supports their involvement in sustaining proteostasis during intense epithelial proliferation and remodeling. Among them, Hsp90 displays nearly double the expression levels observed for the other chaperones, suggesting a particularly prominent role for Hsp90 in stabilizing signaling proteins and cytoskeletal elements required for coordinated epithelial growth during murine salivary gland development.

Developmental studies in other organ systems further emphasize the importance of molecular chaperones in mammalian morphogenesis. Grp78 and Grp94 exhibit high expression during embryonic heart development.[23] Early in embryogenesis, Grp78 is strongly expressed in the neural tube, gut endoderm, somites, and surface ectoderm, whereas Grp94 is predominantly detected in neuroepithelium and surface ectoderm.[23] Knockout models have demonstrated that loss of either Grp78 or Grp94 leads to severe developmental abnormalities, including embryonic lethality due to failure of mesoderm formation or extensive apoptosis of the inner cell mass, respectively, the latter representing the precursor population of embryonic stem cells.[23] At later developmental stages, Hsp27 shows preferential expression in multiple muscle tissues, including the heart, as well as in neurons, spinal cord, bladder, regressing notochord, and lens.[23] Notably, Hsp27 is essential for craniofacial development, as evidenced by the marked inhibition of anterior and middle Meckel's cartilage formation following Hsp25 knockout in E10 embryos.[23] Hsp60 likewise plays a crucial role in early development,

with aberrant expression leading to growth retardation at E6 and embryonic degeneration by E7.5 in mice.[23]

When examined in parallel, the human embryonic data reveal both conserved and distinct features relative to the murine model**.** In the 13-week human embryo, tissue levels of Hsp10, Hsp60, and Hsp90 are markedly elevated compared with murine embryonic glands. This coordinated upregulation suggests an increased requirement for chaperonin-mediated protein folding (Hsp10/Hsp60) and for Hsp90-dependent stabilization of regulatory proteins during the more prolonged and complex timeline of human salivary gland morphogenesis. The prominence of Hsp10 and Hsp60 further supports a role for mitochondrial proteostasis in sustaining the high metabolic demands associated with ductal and acinar differentiation in the human embryo.

In AM Submandibular Gland (SMG), expression of all four chaperones is largely restricted to the ductal compartment, with the notable exception of Hsp90, which maintains substantial expression in both ducts and acini. This pattern suggests that, in mice, Hsp90 continues to support acinar cell function beyond development, potentially reflecting ongoing requirements for protein quality control in secretory cells. In adult human SMG, acinar expression is more pronounced for all Hsps except Hsp27, although ductal localization remains predominant overall. Despite interspecies differences in relative compartmental distribution, the persistence of CS components in ductal structures in both AM and human glands points to a conserved role in maintaining epithelial homeostasis**.** This confinement may relate to the regulation of Na^+/H^+ exchangers, which are critical for salivary pH control and represent a key physiological function of the salivary glands.[12]

In this work gene expression analyses of AM SMG report significant downregulation of Hsp25 compared with Hsp10 and Hsp60. However, our immunohistochemical findings reveal tissue levels of Hsp27 comparable to those of Hsp60. This apparent discrepancy likely reflects methodological differences between transcriptomic and protein-based approaches, as well as species-specific factors, given that murine Hsp25 and human Hsp27 are functional homologues rather than identical proteins. Additional regulatory mechanisms, including post-transcriptional modulation, differential protein stability, or context-dependent degradation, may further contribute to the observed divergence between mRNA and protein expression profiles.

The present study is primarily descriptive in nature, and the results should be interpreted in light of several inherent limitations. First, our observations are based on morphological and molecular analyses and were not supported by functional assays capable of demonstrating a causal role of the investigated factors in the described biological processes. Therefore, the conclusions drawn remain preliminary and will require functional validation in future studies.

Second, the analysis was conducted on a limited number of embryonic stages, which does not allow for a continuous reconstruction of the temporal dynamics of the observed phenomena. Additional developmental windows may reveal quantitative or qualitative variations that were not captured in the present work.

Finally, the limited availability of human embryonic material represents an unavoidable constraint in this field of research and may affect sample size and the generalizability of the findings. Although all possible measures were taken to ensure the robustness and reproducibility of the observations, future studies involving larger cohorts and, where feasible, complementary experimental models will be necessary to confirm and extend our results.

Conclusions

Previous studies mapping the spatial and temporal distribution of major components of the CS, particularly molecular chaperones, across developmental stages have pointed to their potential relevance in both ontogenesis and adulthood. Building on this background, the present study provides the first systematic topographic and quantitative characterization of CS distribution in salivary glands. The distinct expression patterns observed between embryonic and adult tissues highlight developmental stage–related differences in CS localization and abundance. While the present data are primarily descriptive, they generate testable hypotheses and define a reference framework for future functional and mechanistic studies aimed at clarifying the role of the CS in salivary gland morphogenesis, homeostasis, and disease, including congenital malformations.

References

1. Holmberg KV, Hoffman MP. Anatomy, biogenesis and regeneration of salivary glands. Monogr Oral Sci 2014;24:1–13.

2. Sangeetha Priya P, Anitha N, Rajesh E, Masthan K. Embryology and development of salivary gland. Eur J Molec Clin Med 2020;7:764–70.

3. Tucker AS. Salivary gland development. Semin Cell Dev Biol 2007;18:237–44.

4. Larsen M, Yamada KM, Musselmann K. Systems analysis of salivary gland development and disease. Wiley Interdiscip Rev Syst Biol Med 2010;2:670–82.

5. Daverkausen-Fischer L, Motyl-Eisemann M, Draga M, et al. Protein expression pattern of the molecular chaperone Mdg1/ERdj4 during embryonic development. Histochem Cell Biol 2020;154:255–63.

6. Miller DJ, Fort PE. Heat shock proteins regulatory role in neurodevelopment. Front Neurosci 2018;12:821.

7. Scieglinska D, Krawczyk Z, Sojka DR, Gogler-Pigłowska A. Heat shock proteins in the physiology and pathophysiology of epidermal keratinocytes. Cell Stress Chaperones 2019;24:1027–44.

8. Macario AJ, de Macario EC. Chaperone proteins and chaperonopathies. In: Fink G, editor. Stress: physiology, biochemistry, and pathology. Elsevier; 2019: p.135–52.

9. Basset CA, Rappa F, Barone R, et al. The chaperone system in salivary glands: hsp90 prospects for differential diagnosis and treatment of malignant tumors. Int J Mol Sci 2022;23:9317.

10. Basset CA, Cappello F, Rappa F, et al. Molecular chaperones in tumors of salivary glands. J Mol Histol 2020;51:109–15.

11. Dagher JB, Hahn-Townsend CK, Kaimal A, et al. Independent and combined effects of Bisphenol A and Diethylhexyl Phthalate on gestational outcomes and offspring development in Sprague-Dawley rats. Chemosphere 2021;263:128307.

12. Basset CA, Rappa F, Lentini VL, et al. Hsp27 and Hsp60 in human submandibular salivary gland: Quantitative patterns in healthy and cancerous tissues with potential implications for differential diagnosis and carcinogenesis. Acta Histochem 2021;123:151771.

13. Basset CA, Conway de Macario E, Leone LG, et al. The chaperone system in cancer therapies: Hsp90. J Mol Histol 2023;54:105–18.

14. Brocchieri L, Conway de Macario E, Macario AJ. hsp70 genes in the human genome: Conservation and differentiation patterns predict a wide array of overlapping and specialized functions. BMC Evol Biol 2008;8:19.

15. Mukherjee K, Conway de Macario E, Macario AJ, Brocchieri L. Chaperonin genes on the rise: new divergent classes and intense duplication in human and other vertebrate genomes. BMC Evol Biol 2010;10:64.

16. Christians ES, Zhou Q, Renard J, Benjamin IJ. Heat shock proteins in mammalian development. Semin Cell Dev Biol 2003;14:283–90.

17. Bagchi M, Ireland M, Katar M, Maisel H. Heat shock proteins of chicken lens. J Cell Biochem. 2001;82:409–14.

18. Loones MT, Chang Y, Morange M. The distribution of heat shock proteins in the nervous system of the unstressed mouse embryo suggests a role in neuronal and non-neuronal differentiation. Cell Stress Chaperones 2000;5:291–305.

19. Huang L, Mivechi NF, Moskophidis D. Insights into regulation and function of the major stress-induced hsp70 molecular chaperone in vivo: analysis of mice with targeted gene disruption of the hsp70.1 or hsp70.3 gene. Mol Cell Biol 2001;21:8575–91.

20. Barnes JA, Smoak IW. Glucose-regulated protein 78 (GRP78) is elevated in embryonic mouse heart and induced following hypoglycemic stress. Anat Embryol (Berl) 2000;202:67–74.

21. Luo S, Mao C, Lee B, Lee AS. GRP78/BiP is required for cell proliferation and protecting the inner cell mass from apoptosis during early mouse embryonic development. Mol Cell Biol 2006;26:5688–97.

22. Barnes JA, Smoak IW. Immunolocalization and heart levels of GRP94 in the mouse during post-implantation development. Anat Embryol (Berl) 1997;196:335–41.

23. Rupik W, Jasik K, Bembenek J, Widłak W. The expression patterns of heat shock genes and proteins and their role during vertebrate's development. Comp Biochem Physiol A Mol Integr Physiol 2011;159:349–66.

24. Neuer A, Spandorfer SD, Giraldo P, et al. Heat shock protein expression during gametogenesis and embryogenesis. Infect Dis Obstet Gynecol 1999;7:10–6.

25. Bensaude O, Babinet C, Morange M, Jacob F. Heat shock proteins, first major products of zygotic gene activity in mouse embryo. Nature 1983;305:331–3.

26. Parascandolo A, Rappa F, Cappello F, et al. Extracellular superoxide dismutase expression in papillary thyroid cancer mesenchymal stem/stromal cells modulates cancer cell growth and migration. Sci Rep 2017;7:41416.

27. Barone R, Macaluso F, Sangiorgi C, et al. Skeletal muscle Heat shock protein 60 increases after endurance training and induces peroxisome proliferator-activated receptor gamma coactivator 1 α1 expression. Sci Rep 2016;6:19781.

28. Barone R, Rappa F, Macaluso F, et al. Alcoholic liver disease: a mouse model reveals protection by *Lactobacillus fermentum*. Clin Transl Gastroenterol 2016;7:e138.

29. Rappa F, Pitruzzella A, Marino Gammazza A, et al. Quantitative patterns of Hsps in tubular adenoma compared with normal and tumor tissues reveal the value of Hsp10 and Hsp60 in early diagnosis of large bowel cancer. Cell Stress Chaperones 2016;21:927–33.

30. Rappa F, Sciume C, Lo Bello M, et al. Comparative analysis of Hsp10 and Hsp90 expression in healthy mucosa and adenocarcinoma of the large bowel. Anticancer Res 2014;34:4153–9.

31. Waterborg JH, Matthews HR. The Lowry method for protein quantitation. Methods Mol Biol 1994;32:1–4.

32. Eid AA, Gorin Y, Fagg BM, et al. Mechanisms of podocyte injury in diabetes: role of cytochrome P450 and NADPH oxidases. Diabetes 2009;58:1201–11.

33. Livak KJ, Schmittgen TD. Analysis of relative gene expression data using real-time quantitative PCR and the 2(-Delta Delta C(T)) Method. Methods 2001;25:402–8.

34. Matwee C, Kamaruddin M, Betts DH, et al. The effects of antibodies to heat shock protein 70 in fertilization and embryo development. Mol Hum Reprod 2001;7:829–37.

35. Voss AK, Thomas T, Gruss P. Mice lacking HSP90beta fail to develop a placental labyrinth. Development 2000;127:1–11.

Table 1. Primers used for quantitative real-time Polymerase Chain Reaction (PCR).

Gene	Primers' sequence
hsp10	F: 5'-TCACTGTTGAAATGGTGTCACG-3' R: 5'-GTTCAGACATCAGTGGAATGGC-3'
hsp25	F: 5'-TCCGGAGGAACTCAAAGTCAAG-3' R: 5'-TTGCCGTGGACCTCAATCA-3'
hsp60	F: 5'-ACGATCTATTGCCAAGGAGG-3' R: 5'-TCAGGGGTTGTCACAGGTTT-3'
26S	F: 5'-AGGAGAAACAACGGTCGTGCCAAAA-3' R: 5'-GCGCAAGCAGGTCTGAATCGTG-3'

Table 2. Heat Shock Protein (Hsp10, Hsp27, Hsp60, and Hsp90) levels in adult and embryo submandibular salivary glands in human and mouse.

Specimen		Hsp10		Hsp27		Hsp60		Hsp90	
		PPC1	Int	PPC	Int	PPC	Int	PPC	Int
Human submandibular gland									
Adult	Ducts2	96.6	+++	92.6	+++	87.6	++/+++	75.5	+/+++
	Acini	92.5	++/+++	15	++/+++	61	+++	36.7	+/++

Embryo	Acini+ Ducts2	90	+/++	43	++	93	+++	95	+/+++
Mouse submandibular gland									
Adult	Ducts	87.6	+/+++	73.3	+/+++	66.6	+/++	87.3	+++
	Acini	15.6	-/++	5	-	5	-	90	+++
Embryo	Acini+ Ducts2	65	++/+++	47.6	+/+++	40	++/+++	94.6	+++

PPC: percentage of positive cells; Int: reaction intensity. Note: Acini and ducts are not discernible at the embryonic stage.

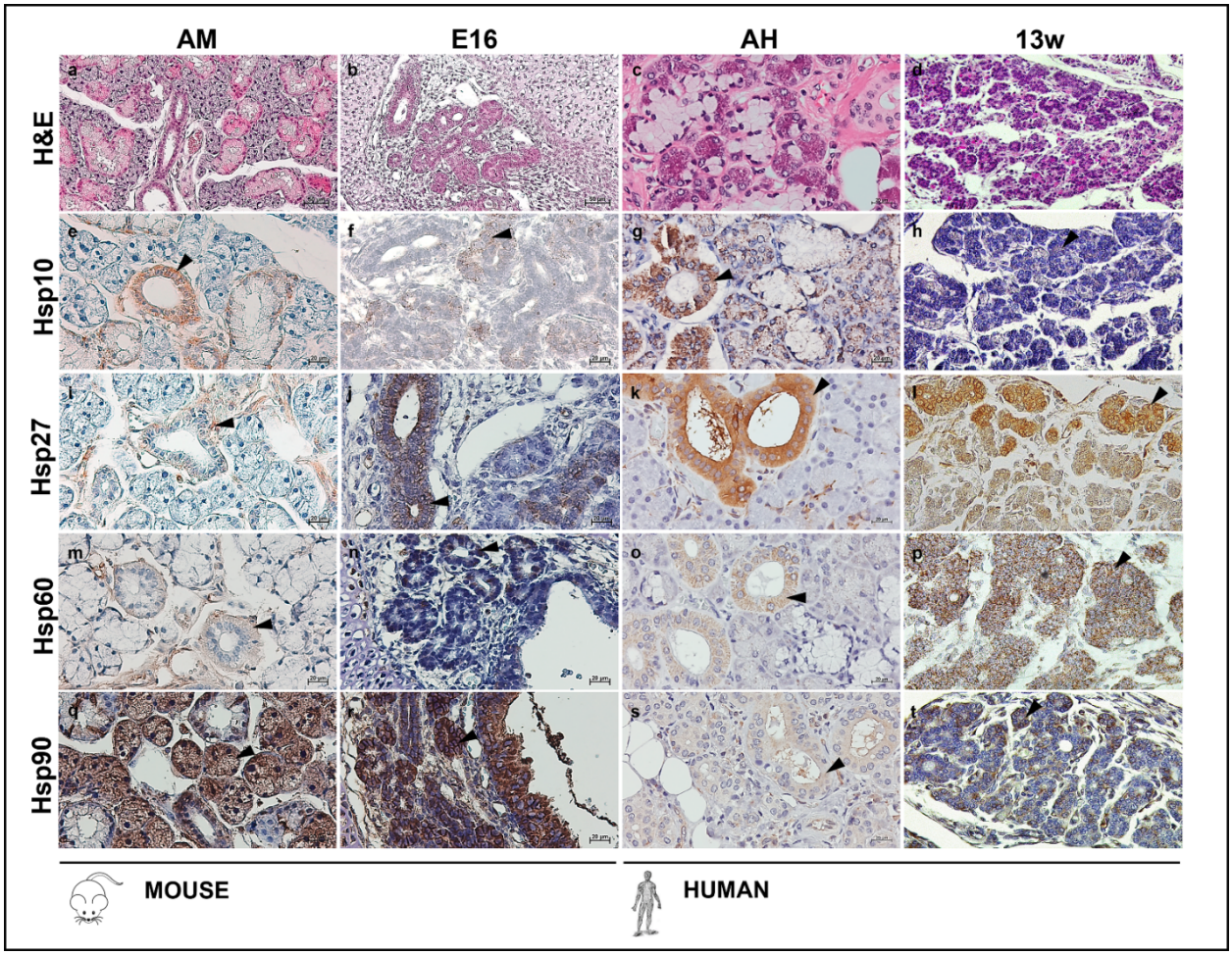

Figure 1. Heat Shock Protein (Hsp10, Hsp27, Hsp60, and Hsp90) tissue levels and distribution in adult and embryonic human and mouse salivary glands. a) Hematoxylin and Eosin (H&E) staining of adult mouse (AM) submandibular gland (SMG). Immunostaining of Hsp10 (e), Hsp27 (i), Hsp60 (m), and Hsp90 (q) in AM SMG (n = 3); b) H&E staining of 16-day gestation mouse embryo (E16). Immunostaining of Hsp10 (f), Hsp27 (j), Hsp60 (n), and Hsp90 (r) in E16 SMG (n = 3); c) H&E staining of adult human (AH) SMG. Immunostaining of Hsp10 (g), Hsp27 (k), Hsp60 (o), and Hsp90 (s) in AH SMG (n = 3); d) H&E staining of 13-week gestation human embryo (13w) SMG. Immunostaining of Hsp10 (h), Hsp27 (l), Hsp60 (p), and Hsp90 (t) in 13w SMG (n = 1). Arrowheads indicate Hsp immunopositivity. Bar = 20 μm.

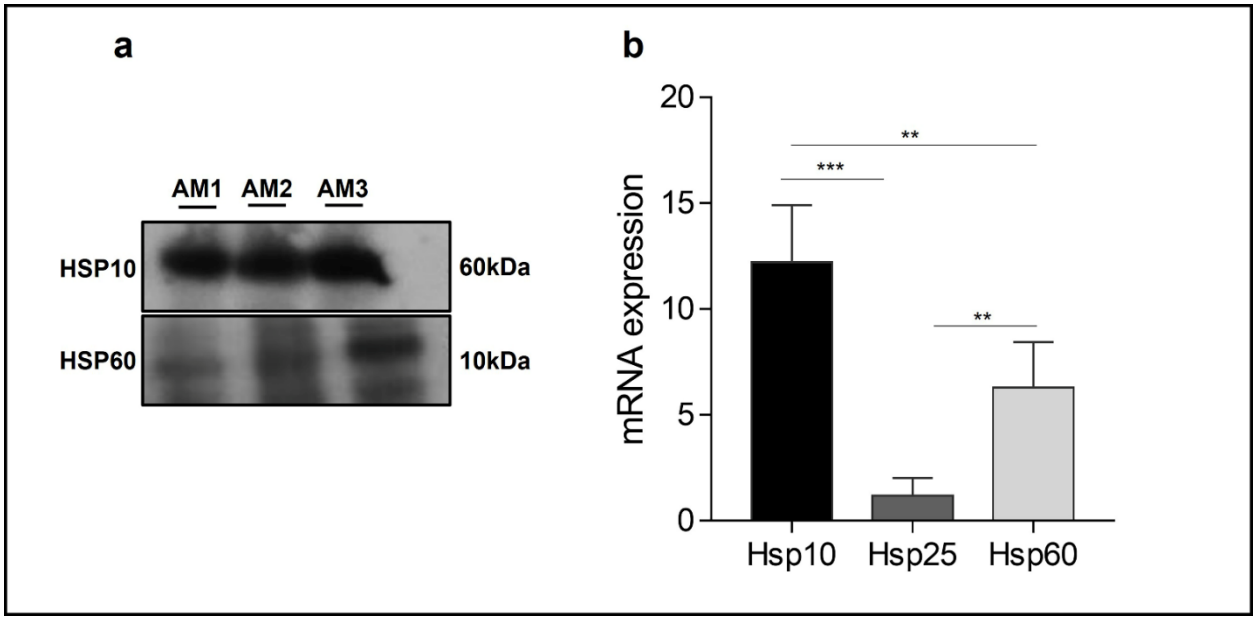

Figure 2. Hsp10, Hsp25, and Hsp60 gene and protein expression levels in adult mouse (AM) Submandibular Gland (SMG). a) Representative Western blot showing Hsp10 and Hsp60 protein expression in AM SMG (n = 3); b) Bar graph depicting mRNA expression levels of Hsp10, Hsp25, and Hsp60 in AM SMG (n = 5). Data are presented as mean ± Standard Deviation (SD). **$p < 0.005$, ***$p < 0.0001$, indicating significant differences

Contributions: Charbel Bassett, erformed the research; Charbel Bassett and Francesca Rappa, acquisition, analysis and interpretation of data; Inaya Hajj Hussein, Laira Dosh, osalyn Jurjus and Abdo Jurjus, provided substantial help with mice experiments; Giuseppe Vergilio, performed WB; Maria Laura Uzzo and Giovanni Francesco Spatola performed IHC experiment; Lavinia Giovanna Leone and Angelo Leone, manuscript drafting and critical revisions; Angelo Leone: Final approval of the version to be published.

Conflict of interest: the authors declare no conflict of interest.

Funding: this research received no external funding.

Ethics approval: not applicable.

Availability of data and materials: all data included in this study are available upon reasonable request by contecting the corresponding author.

Acknowledgements: we would like to formally thank Dr. Marit H. Aure, expert in the salivary gland field, for her critical reading of the manuscript.